Optimization of Switch Diagnostics on the MAIZE Linear Transformer Driver

A. P. Shah,[1, a)] P. C. Campbell,[2] S. M. Miller,[2] J. M. Woolstrum,[2] B. J. Sporer,[2] S. G. Patel,[3] N. M. Jordan,[2] R. M. Gilgenbach,[2] and R. D. McBride[1, 2]

[1)] *Applied Physics Program, University of Michigan, Ann Arbor, Michigan– 48109*

[2)] *Nuclear Engineering and Radiological Sciences Department, University of Michigan, Ann Arbor, Michigan– 48109*

[3)] *Sandia National Laboratories, Albuquerque, New Mexico– 87185*

(Dated: 10 October 2019)

The MAIZE Linear Transformer Driver consists of 40 capacitor-switch-capacitor 'bricks' connected in parallel. When these 40 bricks are charged to ±100-kV and then discharged synchronously, the MAIZE facility generates a 1-MA current pulse with a 100-ns rise time into a matched load impedance. Discharging each of the capacitors in a brick is carried out by the breakdown of a spark-gap switch, a process which results in the emission of light. Monitoring this output light with a fiber optic coupled to a photomultiplier tube (PMT) and an oscilloscope channel provides information on switch performance and timing jitter– whether a switch fired early, late, or in phase with the other switches. However, monitoring each switch with a dedicated detector-oscilloscope channel can be problematic for facilities where the number of switches to be monitored (e.g., 40 on MAIZE) greatly exceeds the number of detector-oscilloscope channels available. The technique of using fibers to monitor light emission from switches can be optimized by treating a PMT as a binary digit or bit and using a combinatorial encoding scheme, where each switch is monitored by a unique combination of fiber-PMT-oscilloscope channels simultaneously. By observing the unique combination of fiber-PMT-oscilloscope channels that are turned on, the pre-firing or late-firing of a single switch on MAIZE can be identified by as few as six PMT-oscilloscope channels. The number of PMT-oscilloscope channels, N, required to monitor X switches can be calculated by $2^N = X + 1$, where the number '2' is selected because the PMT-oscilloscope acts as a bit. In this paper, we demonstrate the use of this diagnostic technique on MAIZE. We also present an analysis of how this technique could be scaled to monitor the tens of thousands of switches proposed for various next generation pulsed power facilities.

I. INTRODUCTION

Pulsed power technology, including Linear Transformer Driver (LTD) technology[1–4], is a cornerstone of high energy density physics (HEDP)[5], supporting applications in nuclear fusion[6–9], material properties[10,11], radiation science[12,13], and laboratory astrophysics experiments[14]. An LTD consists of the parallel connection of fast capacitors and switches around the outer perimeter of a cylindrical cavity (see Fig. 1). These capacitors and switches are grouped together in units called 'bricks' (see Fig. 2). Each brick consists of an upper and lower capacitor charged as high as ±100-kV. The two capacitors are connected in series with each other through the breakdown (closure) of a pressurized spark-gap switch. The MAIZE LTD[15] at the University of Michigan consists of 40 such bricks (Fig. 1). When the bricks are charged to ±100-kV and then discharged synchronously, MAIZE generates a 1-MA current pulse with a 100-ns rise time into a matched load impedance[16].

The capacitors in a brick are rapidly discharged when the switch is closed, driving a current pulse into the experiment of interest. The spark-gap switch is closed by applying a high-voltage pulse to the trigger electrode, which is positioned between the positively charged anode and the negatively charged cathode. All of the electrodes are housed within the switch's pressurized, dielectric body. The applied voltage pulse ionizes the gas, which 'closes' the switch and allows the capacitors to discharge as shown in the equivalent circuit model of a brick in Fig. 2 (bottom). The breakdown of the gas also results in the emission of light, which can be monitored as a proxy for switch performance since the light emitted is temporally correlated with the switch closing.

Monitoring switches by their output light provides information about when the switches first close and thus when the capacitors first begin to discharge. Knowing when each switch closes is crucial for producing the desired current pulse and thus the desired experimental conditions[17]. For example, some experiments require that all the switches close simultaneously, while other experiments require that the switches close at varied, yet predetermined times in order to customize the current pulse delivered to the load[18].

The diagnostic system presented herein is set up such that light from a switch is collected by an optical fiber, which is coupled to a photomultiplier tube (PMT). The PMT converts collected light into a voltage signal, which is monitored by an oscilloscope channel. Monitoring each switch with a dedicated fiber-PMT-oscilloscope channel requires 40 such channels on MAIZE, which was problematic for our laboratory, as 40 PMT-oscilloscope channels were not available. This paper establishes a framework for optimizing a fiber-based switch diagnostics scheme for limited PMT-oscilloscope channels. This is done by assigning each switch to a unique combination of PMTs. A

[a)] Akash Prafulchandra Shah; akashah@umich.edu

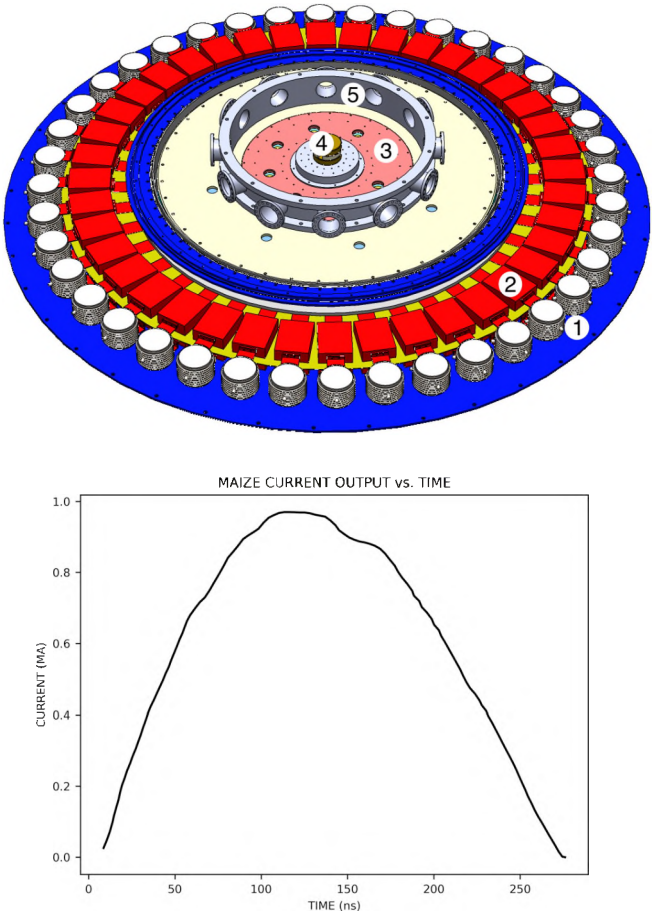

FIG. 1. Top: top view of the 3-m-diameter MAIZE LTD with the outer cavity wall and top lids removed to illustrate the internal components: (1) spark-gap switch– 40 such switches in the LTD; (2) 40 nF capacitor– 80 such capacitors in the LTD; (3) radial transmission line section; (4) load region; and (5) vacuum chamber. Bottom: an example of the discharge current through a matched load impedance on MAIZE, showing an approximately 1-MA current output[16].

pre-firing (or late-firing) switch can then be identified by the unique combination of PMT output pulses.

II. OPERATING THEORY BASED ON BOOLEAN LOGIC

Optimizing switch diagnostics to require fewer PMTs and oscilloscope channels can be accomplished by implementing a logic circuit after light from the switches is collected. In particular, a light circuit can be set up using a network of light-collecting fiber optic cables such that each PMT functions as a binary digit or bit. In this approach, a given PMT is either in an 'on' state (collecting light) or in an 'off' state (not collecting light) at each point in time. Note that a given PMT is in an 'on' state if any one of the switches coupled to the PMT is emitting light, while the PMT is in an 'off' state only if all of the

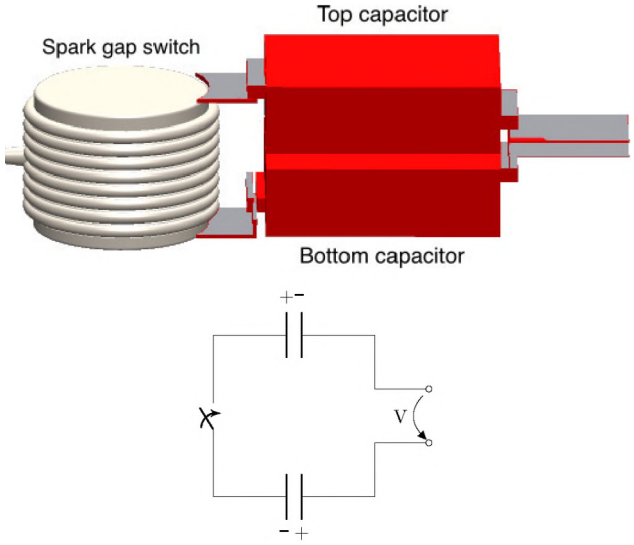

FIG. 2. Top: a gas filled spark-gap switch connected in series with two capacitors to form a 'brick'. Bottom: an equivalent circuit model of a brick.

switches coupled to the PMT are not emitting light.

With N PMTs functioning as bits, one can distinctly represent

$$2^N = X + 1 \tag{1}$$

characters, where X is the number of switches. Given X switches, solving for N provides the minimum number of PMTs required to represent each switch independently. This is shown by

$$N = \lceil \log_2 (X + 1) \rceil \tag{2}$$

where $\lceil\rceil$ is a ceiling function that rounds up its argument, $\log_2 (X + 1)$, to the next whole number. With $X = 40$ switches on MAIZE, the fewest number of PMTs needed to uniquely identify a pre-firing or late-firing switch is $N = 6$.

This diagnostic technique requires coupling each switch to a unique *combination* of PMTs (as opposed to a unique *permutation* of PMTs). A combination of PMTs is a selection of a subset of PMTs from the total, such that the order of selection does not matter– selecting PMT '1' and '2' is the same as selecting PMT '2' and '1'. A permutation of PMTs is a selection where the order does matter– selecting PMT '1' and '2' is *not* the same as selecting PMT '2' and '1'.

With a unique combination of PMTs coupled to each switch, the firing of a single switch can then be identified by the combination of PMTs that are turned on. The available combinations are determined using binomial coefficients,

$$\binom{N}{k} - \frac{N!}{k!(N-k)!} \tag{3}$$

which give the number of ways to choose a subset of k elements from a set of N elements. Each switch is as-

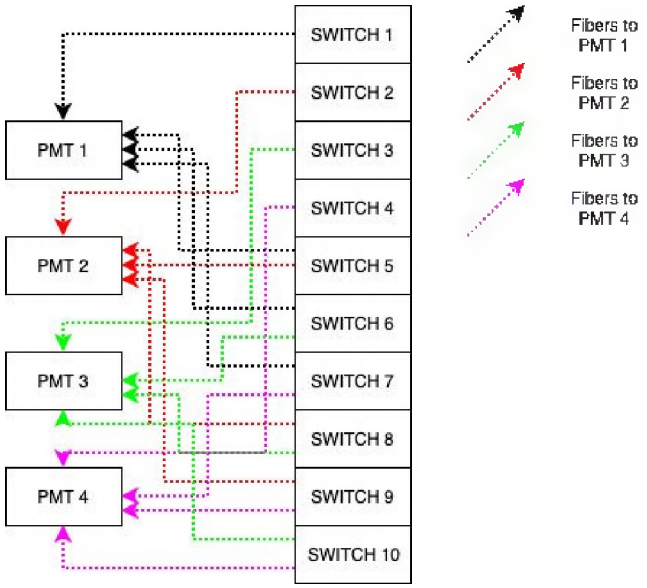

FIG. 3. An example of how four PMT-oscilloscope channels can be used to monitor 10 switches.

signed to one of these combinations. Figure 3 provides an example of what such a circuit would look like in order to monitor ten switches. Note that there is one way to choose 0 elements from a set: $\binom{N}{0} = 1$, which corresponds to assigning a switch to zero PMTs. However, this assignment is not used since it does not actually monitor any switches. This offset in the number of available, practical assignments is accounted for by the '+1' on the right hand side of Eqn. 1.

On MAIZE (having calculated that we need a minimum of six PMTs to monitor 40 switches) there are $\binom{N}{k} = \binom{6}{1} = 6$ ways to choose one PMT, which implies that each of the first six switches get assigned to each of the six PMTs. There are $\binom{N}{k} = \binom{6}{2} = 15$ ways to choose two PMTs, which corresponds to a further 15 switches getting assigned, albeit to two PMTs instead of one. The remaining 19 switches are assigned to three PMTs by choosing three PMTs from the set of six [i.e., $\binom{N}{k} = \binom{6}{3} = 20 > 19$]. In this manner, a minimum of six PMTs allows diagnosis of 40 individual switches. Note that, while only six PMTs are needed, the system implemented on MAIZE uses seven PMTs, since seven PMTs and oscilloscope channels were already available (see Sec. III).

Note that other switch diagnostic schemes could be implemented. For instance, the output light from each switch could be monitored by an inexpensive photodiode, converting the light signal into a digital electrical signal ('0' for no light; '1' for light). The digital signal from each photodiode could then be fed into one of the inputs of a resistor ladder, so that the digital voltage from the first photodiode gets divided by 1, the second by 2, the third by 4, and so on. The total resistor ladder output voltage (the sum of all the scaled photodiode voltages) then uniquely identifies the combination of firing switches. Analyzing the amplitude of the summed signal would then allow pre-firing or late-firing switches to be identified. Mathematically, a resistor ladder of arbitrary length could be constructed such that any number of switches could be monitored using a single ladder-oscilloscope channel. In practice, however, this technique is limited by noise levels on the oscilloscope. Nevertheless, each oscilloscope channel should be able to resolve eight switches, which means that the number of oscilloscope channels required to monitor all 40 switches on MAIZE could be reduced to five. Another benefit of the resistor ladder technique is that there is only one fiber per switch. For these reasons, the resistor ladder solution could be quite useful for smaller facilities like MAIZE. However, we note that the number of oscilloscope channels required to monitor a given number of switches grows linearly with the number of switches to be monitored, which is not as favorable as the logarithmic scaling of the Boolean technique demonstrated in this paper. For example, to monitor 100,000 switches (see Sec. V), a resistor ladder solution might require 12,500 oscilloscope channels, while the Boolean technique demonstrated in this paper could require as few as 17 oscilloscope channels.

III. IMPLEMENTATION ON THE MAIZE FACILITY

Coupling 40 spark-gap switches on MAIZE to unique combinations of PMTs allows for their monitoring using exponentially fewer PMT-oscilloscope channels than monitoring each switch with its own, dedicated PMT-oscilloscope channel. While 40 switches can be monitored with only 6 PMTs (as calculated in Sec. II), the system on MAIZE was implemented with seven PMTs because we already had seven PMT-oscilloscope channels available. As such, we assigned $\binom{N}{k} = \binom{7}{1} = 7$ switches to one PMT; $\binom{N}{k} = \binom{7}{2} = 21$ switches to 21 different combinations of two PMTs; and the remaining 12 switches to 12 combinations of three PMTs [i.e., $\binom{N}{k} = \binom{7}{3} = 35 > 12$]. Table I shows the PMT assignments for the 40 switches on MAIZE. Note that the total number of fibers is dependent on the number of switches in the LTD, the number of PMTs used to monitor the switches, and how the PMTs are assigned to the switches. This number can grow rapidly, and meticulous cable management becomes a necessity. Additional analysis of this issue is presented in Sec. V.

We used roughly 18 m of 1-mm-diameter step-indexed multimode fiber optic cable to couple each switch to its respective combination of PMTs. The fibers were attached to the switches using 3D-printed fiber holders, where each holder had an elongated support structure, which was fitted into a feedthrough port in the spark-gap switch's dielectric housing. These holders also provide fiber strain relief, which reduces the chances of a fiber breaking. This is useful because the setup does not

TABLE I. PMT Assignments on MAIZE

SWITCH	PMT(s)	SWITCH	PMT(s)
1	1	21	3,6
2	2	22	3,7
3	3	23	4,5
4	4	24	4,6
5	5	25	4,7
6	6	26	5,6
7	7	27	5,7
8	1,2	28	6,7
9	1,3	29	1,2,3
10	1,4	30	1,2,4
11	1,5	31	1,2,5
12	1,6	32	1,2,6
13	1,7	33	1,3,4
14	2,3	34	1,3,7
15	2,4	35	2,3,5
16	2,5	36	4,5,6
17	2,6	37	4,5,7
18	2,7	38	3,6,7
19	3,4	39	4,6,7
20	3,5	40	5,6,7

detect damaged fibers. For switches that are assigned to multiple PMTs, we used a dedicated fiber for each switch-PMT connection. This means that each switch had one, two, or three fibers residing in its feedthrough port, which required running 85 fibers in total from the MAIZE LTD cavity to the PMT box in the MAIZE screen room. The PMTs were housed within a light-tight Faraday cage to minimize electromagnetic interference from potential noise sources.

The system is triggered by the first switch that fires. This is done so that the oscilloscopes can be set to record waveforms with nanosecond resolution while also continually monitoring for pre-firing switches during the charging of the LTD, which can take several tens of seconds. To enable this triggering scheme, we split the output of each of the seven PMTs into two lines (see Fig. 4). One of the lines connects to the input of an oscilloscope channel, while the other line connects to one of the inputs of an eight-channel adder (of which we only used seven channels). We used a 1N4148 diode between the PMT outputs and the adder inputs to isolate the PMT outputs from each other (i.e., without the diodes, the PMT outputs are shorted together in the adder circuit). The 1N4148 diode was selected because of its sufficiently low forward bias voltage (allowing signals to propagate relatively unimpeded in the forward direction) and because of its sufficiently large backwards bias voltage (isolating the PMT outputs from each other). We then split the adder output into two trigger signals, one for each four-channel oscilloscope.

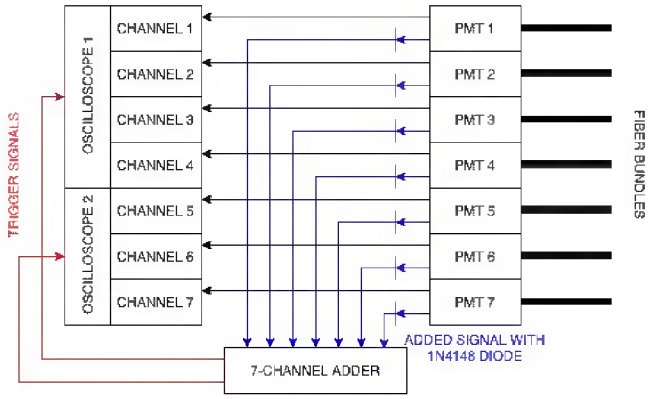

FIG. 4. A schematic of the experimental setup to monitor the 40 switches on MAIZE.

IV. RESULTS ON THE MAIZE FACILITY AND POTENTIAL FUTURE IMPROVEMENTS

The diagnostic configuration described in Sec. III is now routinely used on MAIZE to identify both single pre-firing and single late-firing switches, while using only seven PMT-oscilloscope channels (see Fig. 5). In Fig. 5 (top), we present the case where all of the switches fire synchronously, thus all of the PMTs turn on at the same time, which indicates proper firing of the LTD. By contrast, in Fig. 5 (bottom), we present the case where switch '27' pre-fires, which, in accordance with Table I, is indicated by PMTs '5' and '7' turning on before the others. For the results presented above, the switches were filled to 95 psig with "Ultra Zero Grade" dry air, the bricks were charged to ± 70 kV, and the load was a short-circuit metal rod.

While this diagnostics scheme works as intended for identifying single switches firing early or very late relative to the rest of the switches, our present implementation has trouble distinguishing which switches closed first when multiple switches pre-fire or late-fire at nearly the same time. For example, switches '5' and '7' pre-firing at the same time would result in a graph similar to Fig. 5 (bottom). Thus, time resolution is important, including both the oscilloscope sampling rate and the PMT detector response. With sufficient time resolution (sub-ns), identifying the first switch to pre-fire should still be possible, as it is very unlikely that multiple switches pre-fire at *exactly* the same time during a relatively long charging sequence (which occurs over many tens of seconds on MAIZE). Additionally, monitoring *calibrated* PMT output amplitudes should allow us to distinguish between a single switch pre-firing (lower PMT output amplitudes) and multiple switches pre-firing at the same time (higher PMT output amplitudes). This would also allow us to identify problematic non-firing switches. Such a diagnostic scheme could be simplified by digitizing the light output from the switches (e.g., using inexpensive photodiodes) instead of relying on calibrated PMTs. We also note that implementing the resistor ladder technique

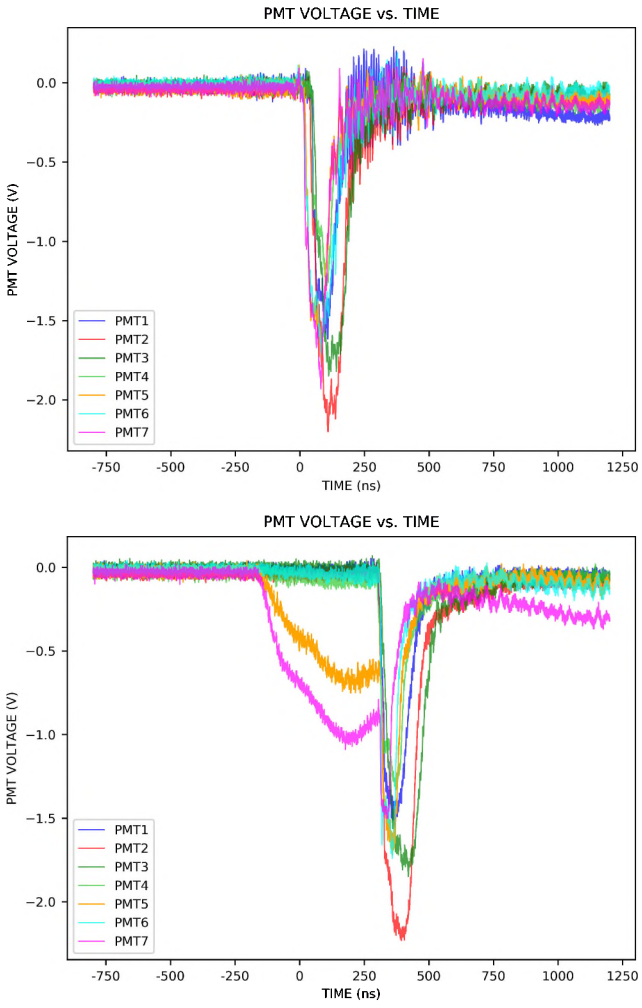

FIG. 5. Top: ideal functioning of MAIZE where all 40 switches fire at the same time. Bottom: a pre-fire in switch '27', as indicated by the early signal received by PMTs '5' and '7', which correspond to the combination of PMTs assigned to switch '27' (*cf.* Table I).

mentioned in Sec. II could help to resolve issues with multiple switches pre-firing at the same time.

The fiber-based techniques described in this paper could give false-positive results for pre-firing switches if a significant amount of light is collected by the fibers from sources other than the switches (e.g., from oil arcs). These issues can be mitigated by shielding and collimating the fibers such that they collect light only from the switches. We intend to implement better shielding and collimation in future implementations on MAIZE. Another potential improvement for this diagnostic is the development of machine learning tools. These tools would be trained on known data sets and could be used to differentiate between single misfiring switches, multiple misfiring switches, and spurious signals (e.g., oil arcs). Such tools would be particularly useful for implementing this diagnostic on large-scale facilities, where tens of thousands of switches may need to be monitored.

V. SCALING SWITCH MONITORING SOLUTIONS TO LARGE PULSED POWER FACILITIES

The diagnostic technique presented in this paper allows for monitoring of X switches by $< X$ PMT-oscilloscope channels. One trade-off in reducing the number of PMT-oscilloscope channels to $< X$ is that the total number of optical fibers that must be routed in the system grows to a number $> X$.

In Fig. 6, we illustrate how the total number of required fibers scales with the number of switches monitored and the number of PMT-oscilloscope channels used. The straight diagonal blue line represents both the number of PMT-oscilloscope channels and the total number of fibers needed when every switch is monitored using an independent fiber-PMT-oscilloscope channel (a 1:1 monitoring scheme). By contrast, the red line is a plot of Eqn. 2, which represents a system using the minimum number of PMT-oscilloscope channels. Note that the red line is the lower bound and the blue line is the upper bound for the overall solution space shaded in red, which represents the range in the number of PMT-oscilloscope channels that could be used to monitor a given number of switches, X. Each point in the lower shaded region (red) corresponds to a point in the upper shaded region (green). The green shaded region represents the range in the total number of optical fibers required to monitor X switches. Note that the upper bound for the green region (the green line) corresponds to the lower bound for the red region (the red line). Also note that, to our knowledge, there is no simple analytic function for calculating the fiber scaling represented by the green line. Thus, we wrote a simple computer algorithm to automate the fiber counting and generate the plot.

In analyzing Fig. 6, a useful heuristic is to recognize that the closer the system is to the red line, the closer it will be to the green line. Similarly, the further the system is from the red line, the further it will be from the green line, until the solutions in the upper and lower shaded regions ultimately converge on the 1:1 monitoring scheme represented by the straight diagonal blue line. This illustrates the trade-off whereby using fewer PMT-oscilloscope channels requires a greater total number of fibers to be routed in the system. For example, the minimum number of PMTs required to monitor the 40 switches on MAIZE is six, as calculated by Eqn. 2. Using this solution would require a total of 93 fibers to be run into the LTD cavity. In Fig. 6, for the case of $X = 40$ switches, the points corresponding to six PMT-oscilloscope channels and 93 fibers lie on the red and green lines, respectively. In our implementation on MAIZE, however, we chose to use seven PMTs instead of six, which then required only 85 fibers total. In Fig. 6, and again for the case of $X = 40$ switches, the points corresponding to seven PMT-oscilloscope channels and 85

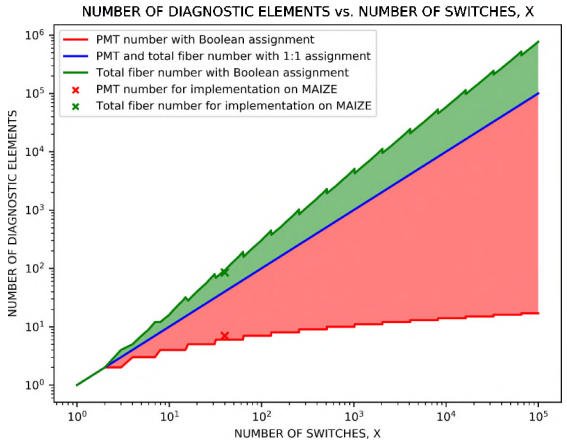

FIG. 6. The solution space for the number of PMT-oscilloscope channels needed and the total number of fibers needed as a function of the number of spark-gap switches to be monitored. The lower bound for the red shaded region (the red line) is given by Eq. 2, which represents the minimum number of PMT-oscilloscope channels needed for monitoring X switches. This solution requires the maximum number of fibers, which is indicated by the green line (the upper bound of the green shaded region). The red and green shaded regions represent intermediate solutions, where extra PMT-oscilloscope channels are employed in order to use fewer fibers. The red and green solution spaces converge on each other at the straight diagonal blue line, which represents a 1:1 monitoring scheme, where every switch is monitored by a dedicated fiber-PMT-oscilloscope channel (i.e., the number of fibers used equals the number of PMT-oscilloscope channels used, which equals the number of switches monitored).

fibers lie in the red and green shaded areas, respectively. If we continued adding more PMT-oscilloscope channels to the system, then the total number of fibers required would continue to decrease until the system eventually converged on the 1:1 scheme, where $X = 40$ switches requires 40 PMT-oscilloscope channels and 40 fibers in total. Indeed, researchers working at large pulsed power facilities might not necessarily want to use the minimum number of PMT-oscilloscope channels; instead, they may want to use more PMT-oscilloscope channels to gain the advantage of using fewer fiber optic cables. Finding a suitable compromise between the number of PMTs used and the number of fibers used depends on the goals of the facility and on the resources available at the facility.

The switch monitoring diagnostic presented in this paper could be useful for next generation pulsed power facilities, where the number of switches to be monitored may be large. For example, some candidate architectures for replacing today's Z facility at Sandia National Laboratories include LTD-based designs with approximately 100,000 switches[19]. Referring to the solution space available for $X = 100{,}000$ switches in Fig. 6, the diagnostic elements needed range from 17 PMT-oscilloscope channels and 768,001 fiber optic cables (with a Boolean scheme) to 100,000 PMT-oscilloscope channels and 100,000 fiber optic cables (with a 1:1 scheme). The diagnostic technique presented in this paper could significantly reduce the resources needed by finding a solution that uses a suitable number of PMT-oscilloscope channels along with a suitable number of fibers.

ACKNOWLEDGMENTS

We would like to thank the anonymous reviewers for their valuable feedback, which helped ensure the completeness of this work. We would also like to thank one of the reviewers for suggesting the alternative approach of using photodiodes with a resistor ladder, which we will be sure to try in the future.

This work was supported in part by the U.S. Nuclear Regulatory Commission through a faculty development grant, in part by a seed grant from the Michigan Memorial Phoenix Project, in part by the National Science Foundation through the NSF-DOE Partnership in Basic Plasma Science and Engineering under Grant PHY-1705418, in part by the DOE-NNSA through the SSAA Program under Cooperative Agreement DE-NA0003764, in part by the ONR through the Young Investigator Program under Grant N00014-18-1-2499, and in part by Sandia National Laboratories through the LDRD and Campus Executives Programs under Project 20-9240. Sandia is a multimission laboratory managed and operated by National Technology and Engineering Solutions of Sandia, LLC., a wholly owned subsidiary of Honeywell International, Inc., for the DOE-NNSA under contract DE-NA0003525.

[1] B. M. Koval'chuk, V. A. Vizir', A. A. Kim, E. V. Kumpyak, S. V. Loginov, A. N. Bastrikov, V. V. Chervyakov, N. V. Tsoi, P. Monjaux, and D. Kh'yui, Russian Physics Journal **40**, 1142 (1997).

[2] A. A. Kim, B. M. Kovalchuk, E. V. Kumpjak, and N. V. Zoi, in *Digest of Technical Papers. 12th IEEE International Pulsed Power Conference. (Cat. No.99CH36358)*, Vol. 2 (1999) pp. 955–958.

[3] A. A. Kim, M. G. Mazarakis, V. A. Sinebryukhov, B. M. Kovalchuk, V. A. Visir, S. N. Volkov, F. Bayol, A. N. Bastrikov, V. G. Durakov, S. V. Frolov, V. M. Alexeenko, D. H. McDaniel, W. E. Fowler, K. LeChien, C. Olson, W. A. Stygar, K. W. Struve, J. Porter, and R. M. Gilgenbach, Phys. Rev. ST Accel. Beams **12**, 050402 (2009).

[4] J. D. Douglass, B. T. Hutsel, J. J. Leckbee, T. D. Mulville, B. S. Stoltzfus, M. L. Wisher, M. E. Savage, W. A. Stygar, E. W. Breden, J. D. Calhoun, M. E. Cuneo, D. J. De Smet, R. J. Focia, R. J. Hohlfelder, D. M. Jaramillo, O. M. Johns, M. C. Jones, A. C. Lombrozo, D. J. Lucero, J. K. Moore, J. L. Porter, S. D. Radovich, S. A. Romero, M. E. Sceiford, M. A. Sullivan, C. A. Walker, J. R. Woodworth, N. T. Yazzie, M. D. Abdalla, M. C. Skipper, and C. Wagner, Phys. Rev. Accel. Beams **21**, 120401 (2018).

[5] R. D. McBride, W. A. Stygar, M. E. Cuneo, D. B. Sinars, M. G. Mazarakis, J. J. Leckbee, M. E. Savage, B. T. Hutsel, J. D. Douglass, M. L. Kiefer, B. V. Oliver, G. R. Laity, M. R. Gomez, D. A. Yager-Elorriaga, S. G. Patel, B. M. Kovalchuk, A. A. Kim, P. . Gourdain, S. N. Bland, S. Portillo, S. C. Bott-Suzuki, F. N. Beg, Y. Maron, R. B. Spielman, D. V. Rose, D. R. Welch, J. C. Zier, J. W. Schumer, J. B. Greenly, A. M. Covington, A. M.

Steiner, P. C. Campbell, S. M. Miller, J. M. Woolstrum, N. B. Ramey, A. P. Shah, B. J. Sporer, N. M. Jordan, Y. Y. Lau, and R. M. Gilgenbach, IEEE Transactions on Plasma Science **46**, 3928 (2018).

[6] S. A. Slutz, M. C. Herrmann, R. A. Vesey, A. B. Sefkow, D. B. Sinars, D. C. Rovang, K. J. Peterson, and M. E. Cuneo, Physics of Plasmas **17**, 056303 (2010), https://doi.org/10.1063/1.3333505.

[7] M. E. Cuneo, M. C. Herrmann, D. Sinars, S. Slutz, W. A. Stygar, R. A. Vesey, A. Sefkow, G. A. Rochau, G. A. Chandler, J. E. Bailey, J. L. Porter, R. McBride, D. C. Rovang, M. G. Mazarakis, E. P. Yu, D. Lamppa, K. Peterson, C. Nakhleh, S. Hansen, and M. Matzen, IEEE Transactions on Plasma Science **40**, 3222 (2012).

[8] S. A. Slutz and R. A. Vesey, Phys. Rev. Lett. **108**, 025003 (2012).

[9] M. R. Gomez, S. A. Slutz, A. B. Sefkow, D. B. Sinars, K. D. Hahn, S. B. Hansen, E. C. Harding, P. F. Knapp, P. F. Schmit, C. A. Jennings, T. J. Awe, M. Geissel, D. C. Rovang, G. A. Chandler, G. W. Cooper, M. E. Cuneo, A. J. Harvey-Thompson, M. C. Herrmann, M. H. Hess, O. Johns, D. C. Lamppa, M. R. Martin, R. D. McBride, K. J. Peterson, J. L. Porter, G. K. Robertson, G. A. Rochau, C. L. Ruiz, M. E. Savage, I. C. Smith, W. A. Stygar, and R. A. Vesey, Phys. Rev. Lett. **113**, 155003 (2014).

[10] R. W. Lemke, D. H. Dolan, D. G. Dalton, J. L. Brown, K. Tomlinson, G. R. Robertson, M. D. Knudson, E. Harding, A. E. Mattsson, J. H. Carpenter, R. R. Drake, K. Cochrane, B. E. Blue, A. C. Robinson, and T. R. Mattsson, Journal of Applied Physics **119**, 015904 (2016), https://doi.org/10.1063/1.4939675.

[11] M. R. Martin, R. W. Lemke, R. D. McBride, J. P. Davis, D. H. Dolan, M. D. Knudson, K. R. Cochrane, D. B. Sinars, I. C. Smith, M. Savage, W. A. Stygar, K. Killebrew, D. G. Flicker, and M. C. Herrmann, Physics of Plasmas **19**, 056310 (2012), https://doi.org/10.1063/1.3694519.

[12] J. E. Bailey, G. A. Chandler, D. Cohen, M. E. Cuneo, M. E. Foord, R. F. Heeter, D. Jobe, P. W. Lake, J. J. MacFarlane, T. J. Nash, D. S. Nielson, R. Smelser, and J. Torres, Physics of Plasmas **9**, 2186 (2002), https://doi.org/10.1063/1.1459454.

[13] G. A. Rochau, J. E. Bailey, Y. Maron, G. A. Chandler, G. S. Dunham, D. V. Fisher, V. I. Fisher, R. W. Lemke, J. J. MacFarlane, K. J. Peterson, D. G. Schroen, S. A. Slutz, and E. Stambulchik, Phys. Rev. Lett. **100**, 125004 (2008).

[14] G. A. Rochau, J. E. Bailey, R. E. Falcon, G. P. Loisel, T. Nagayama, R. C. Mancini, I. Hall, D. E. Winget, M. H. Montgomery, and D. A. Liedahl, Physics of Plasmas **21**, 056308 (2014), https://doi.org/10.1063/1.4875330.

[15] R. M. Gilgenbach, M. R. Gomez, J. C. Zier, W. W. Tang, D. M. French, Y. Y. Lau, M. G. Mazarakis, M. E. Cuneo, M. D. Johnston, B. V. Oliver, T. A. Mehlhorn, A. A. Kim, and V. A. Sinebryukhov, AIP Conference Proceedings **1088**, 259 (2009), https://aip.scitation.org/doi/pdf/10.1063/1.3079742.

[16] M. R. Gomez, *Experimental Examination of Plasma Formation and Current Loss in Post-Hole Convolutes*, Ph.D. thesis, University of Michigan (2011).

[17] A. M. Steiner, D. A. Yager-Elorriaga, S. G. Patel, N. M. Jordan, R. M. Gilgenbach, A. S. Safronova, V. L. Kantsyrev, V. V. Shlyaptseva, I. Shrestha, and M. T. Schmidt-Petersen, Physics of Plasmas **23**, 101206 (2016), https://doi.org/10.1063/1.4965241.

[18] E. M. Waisman, D. B. Reisman, B. S. Stoltzfus, W. A. Stygar, M. E. Cuneo, T. A. Haill, J.-P. Davis, J. L. Brown, C. T. Seagle, and R. B. Spielman, Review of Scientific Instruments **87**, 063906 (2016), https://doi.org/10.1063/1.4954173.

[19] W. A. Stygar, T. J. Awe, J. E. Bailey, N. L. Bennett, E. W. Breden, E. M. Campbell, R. E. Clark, R. A. Cooper, M. E. Cuneo, J. B. Ennis, D. L. Fehl, T. C. Genoni, M. R. Gomez, G. W. Greiser, F. R. Gruner, M. C. Herrmann, B. T. Hutsel, C. A. Jennings, D. O. Jobe, B. M. Jones, M. C. Jones, P. A. Jones, P. F. Knapp, J. S. Lash, K. R. LeChien, J. J. Leckbee, R. J. Leeper, S. A. Lewis, F. W. Long, D. J. Lucero, E. A. Madrid, M. R. Martin, M. K. Matzen, M. G. Mazarakis, R. D. McBride, G. R. McKee, C. L. Miller, J. K. Moore, C. B. Mostrom, T. D. Mulville, K. J. Peterson, J. L. Porter, D. B. Reisman, G. A. Rochau, G. E. Rochau, D. V. Rose, D. C. Rovang, M. E. Savage, M. E. Sceiford, P. F. Schmit, R. F. Schneider, J. Schwarz, A. B. Sefkow, D. B. Sinars, S. A. Slutz, R. B. Spielman, B. S. Stoltzfus, C. Thoma, R. A. Vesey, P. E. Wakeland, D. R. Welch, M. L. Wisher, and J. R. Woodworth, Phys. Rev. ST Accel. Beams **18**, 110401 (2015).